Factors Influencing the Tangential AC Breakdown Strength of Solid-Solid Interfaces

Emre Kantar, Dimitrios Panagiotopoulos and **Erling Ildstad**
Department of Electric Power Engineering
Norwegian University of Science and Technology
Trondheim, 7491, Norway

ABSTRACT

The combination of two solid dielectrics (interface) increases the risk of formation of microscopic cavities reducing the breakdown strength (BDS) of the interface considerably, particularly when the electric field has a tangential component. The main purpose of this paper is to investigate the impact of the applied contact pressure and composite elastic modulus on the tangential ac BDS of the solid-solid interfaces experimentally. In the experiments, three different contact pressures were applied using different mechanical loads with two different materials having different elastic moduli, i.e. cross-linked polyethylene (XLPE) and silicon rubber (SiR). Two rectangular prism shaped samples were placed between two vertical Rogowski shaped electrodes either in air or oil. The type of the interface (air/oil) is highlighted duly upon showing the results. Increase in contact pressure caused relatively higher increase in the tangential BDS of dry SiR-SiR (assembled in air) than that of XLPE-XLPE, revealing that elastic modulus facilitated significantly to reduce the mean void size in SiR that in turn improved the tangential BDS. Likewise, the tangential BDS of hybrid interfaces formed by XLPE-SiR specimens increased by 43% compared to that of XLPE-XLPE interface at the same pressure. Additionally, the same set of experiments assembled in oil reveals that the presence of oil enhanced the tangential BDSs around 2-3 times for all three-interface cases. Moreover, with the increase of applied pressure the tangential BDS of air-filled and oil-filled cavities tended to get significantly higher.

Index Terms— **Cable insulation, dielectric breakdown strength, elastic modulus.**

1 INTRODUCTION

SUBSEA cable connectors are vital components of oil and gas installations and of future ocean renewable energy systems. They allow quick, reliable and in situ connection of offshore modules to main components while they provide versatility and modularity of expensive equipment and cables where in some cases total system design is dictated by availability of connector technology [1, 2]. Usually a distinction between subsea cable connectors is made according to their type, such as wet-mate connectors, dry-mate connectors and penetrators. Wet-mate connectors are gaining a position in renewable industry nowadays (offshore wind farms, tidal energy systems, etc.) and have already been used in oil and gas industry for years due to ease in plugging underwater [1-5]. However, recent and future subsea extensions stipulate significant and cost-effective developments in wet-mate connector technologies, which should be able to withstand and operate under higher voltage levels/power ratings, higher temperatures, deeper waters and longer tiebacks [1, 3]. Nowadays, wet-mate cable connectors up to 36 kV are commercially available but the connectors up to 150 kV should be available within the next decade to fulfill the driving force to provide more power [1, 2]. Consequently, wet-mate cable terminations/connectors constitute very critical components in the power supply system and the majority of direct failures are related to such components. To tackle with these failures and to fulfill the growing demands of industry, weak parts of the connections, one of which is the solid-solid interface in this case [1], must be examined quite in detail.

An inherent problem of any cable connector and termination is the presence of interfaces between materials. If the breakdown strength at a point on the interface is exceeded by local field enhancement, partial discharges will be initiated [6]. Since the combination of two solid dielectrics increases the risk of existence of microscopic cavities and imperfections on the interface, reducing the breakdown strength (BDS) of the interface considerably, particularly when the electric field has a tangential (longitudinal) component [3-5, 7]. Figure 1a shows a wet-mate connector and where the interface is formed whereas Figures 1b and 1c provides a closer look on the interface asperities by the simplified profile of contact asperities using an ideally flat and a rigid surface (equivalent to two rigid surfaces [8]). The main failure type of such interfaces is the tracking failure defined as the formation of a conductive path. Even though the magnitude of electric field is

Manuscript received on 24 November 2015, in final form 13 January 2016, accepted 13 January 2016.

much lower compared to the dielectric strength of the bulk insulation, the existence of the microscopic cavities (see Figure 1) and imperfections (contaminant and water droplets) at the interface cause electric field enhancement. The field enhancement might result in initiation of partial discharge (PD) and when the discharges persist for a considerable time, the discharge energy induces carbon decomposition on the surfaces. Eventually, the carbonized deposits bridge the electrodes and breakdown (BD) follows immediately [3-5].

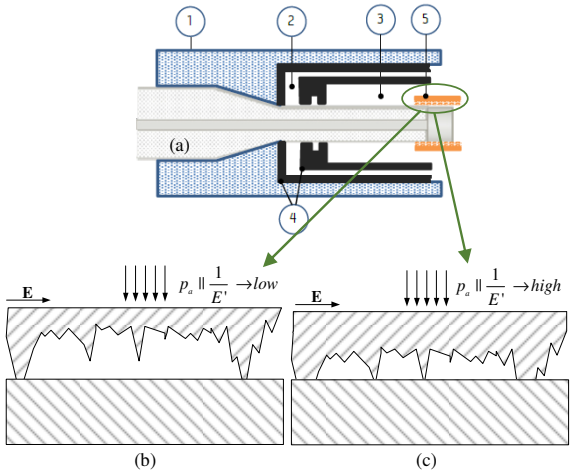

Figure 1. (a) Schematic drawing of a wet-mate connector plug. (1) Insulated polymer housing (2) Outer oil volume (3) Inner oil volume (4) Viper seals (5) Tulip contact. (b-c) Texture of a solid-solid interface consisting of contact spots and asperities (b) Low p_a or high E' (c) High p_a or low E'.

Applied contact pressure (p_a), surface roughness (R) and the composite elastic modulus (a.k.a. Young's modulus) of the interface (E') are the key parameters affecting the size and number of voids on contact surface that in turn affects the tangential ac BDS of the interface [3-5, 7, 9-13]. The composite elastic modulus E' expresses the aggregate elastic modulus E of the combination of the two materials [8]. The properties of the dielectric medium filling the cavities (air, water, oil, extraneous particles, etc.) has also a substantial impact on the BDS of the interface. Figure 2 reveals all the parameters of concern with their interdependency.

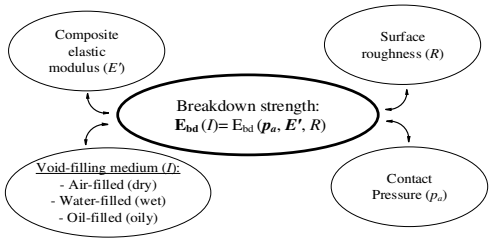

Figure 2. Conceptual diagram depicting the parameters having an influence on solid-solid interfacial breakdown strength.

Great amount of research has been dedicated to the study of insulating materials, their breakdown strength and their applications in power engineering (cables, accessories, etc.). However, very little is known about the characteristics of solid-solid interfaces as they appear in cable joints and connectors which are the key components that secure the long service life in diverse environments [2, 7, 10-13]. The majority of research articles are restricted to study complete designs of connectors/joints without exercising due care on the interface [1]. The breakdown along the interface of solid insulation is a complex phenomenon, which is yet not fully investigated and explained [10]. Therefore, the specific parameters that influence the breakdown of solid-solid interfaces when the field is applied tangentially to the interface must be studied separately [7, 10-13]. Several studies in the literature examined the effect of contact pressure and surface roughness on the tangential BDS and reported that the higher interfacial pressure and smoother surfaces lead to higher breakdown strength [3-5, 7, 10-13]. There are, however, many vague points raising the following questions: What is the impact of the contact pressure on the BDS of interfaces formed by a softer material (i.e. lower elastic modulus)? How the elastic modulus is expected to affect the BDS of the interface? How is the BDS of the interface affected when combining a hybrid interface (i.e. soft-hard combination of materials) which is the case in practice/in a real connector (Figure 1a)? How does the ingress of oil in the interface affect the BDS of different materials having distinct elasticity moduli? To find appropriate answers to the raised questions, the main purpose of this paper is to investigate the impact of the contact pressure, the composite elastic modulus and the dielectric strength of the void-filling medium on the tangential BDS of the solid-solid interfaces experimentally. Surface roughness is kept constant in this study while three different contact pressures with two different solid materials having different elastic moduli, namely cross-linked polyethylene (XLPE) and silicon rubber (SiR). To realize the impact of the void-filling medium on the dielectric strength, air-filled and oil-filled (lubricated/oily interface) void cases are contrasted by repeating the same set of experiments using samples with definite volume of oil injected on the interface.

In the following, first, a theoretical approach considering the distribution of contact spots and voids formed in dry interfaces is employed to build a basis for the interpretations of the experimental results. Second, the test setup and adopted experiment procedure together with the specimen preparation methods are described and then the ac breakdown test results of dry interfaces (for XLPE-XLPE, SiR-SiR and XLPE-SiR interfaces) are presented. Last, the tangential BDS difference between air-filled and oil-filled cavities is analyzed experimentally and conclusions are given in the end.

2 MODELING THE INTERFACE

In this section, a contact model developed in [3] is used to describe the voltage distribution across voids and contact spots at the interface.

2.1 BREAKDOWN VOLTAGE OF A DRY INTERFACE

When there is a contact surface between solids, voids and contact spots are formed at the dry interface due to surface asperities as shown in Figure 1. As seen in Figure 1a, the taller summits have contact with the surface first and large cavities are formed on the interface. In contrast, as seen in Figure 1b, if the material is softer (lower E' or higher $1/E'$), the tall summits

can be compressed further and more summits reach the flat surface. As a result, there are now smaller cavities. Considering the Paschen's curves in Figure 3, having smaller cavities means smaller air gaps and thus higher breakdown strength over a longer total distance. Therefore, the interface made of a softer material is expected to be able to withstand higher applied voltage. Similarly, the influence of increasing the mechanical force/contact pressure pushes the tall summits further yielding smaller voids, increasing the gas pressure inside the voids and hence higher breakdown strength is obtained. Thus, this equivalent impact of p_a and $1/E'$ is revealed in Figure 1. Likewise, assumption of a high degree of surface roughness would result in fewer but larger voids (as in Figure 1a) yet, surface roughness parameters are fixed that will be identical for each material individually in each experiment.

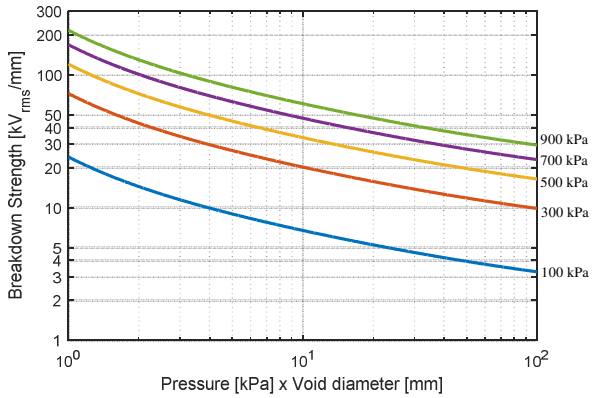

Figure 3. Breakdown strength of spherical air gaps as a function of the *pd* [kPa·mm].

2.2 SIMPLIFIED DRY INTERFACE MODEL

Series connections of voids and contact spots construct a simplified model of the interface where the applied voltage is distributed along the interface according to

$$V_a = \sum_{k=1}^{n} V_{k,void} + \sum_{l=1}^{n} V_{l,contact} \qquad (1)$$

where V_a is the applied voltage across the dry interface, $V_{k,void}$ is the voltage drop across i^{th} void, and $V_{l,contact}$ is the voltage drop across l^{th} contact spot located between two voids as shown in Figure 4 [3].

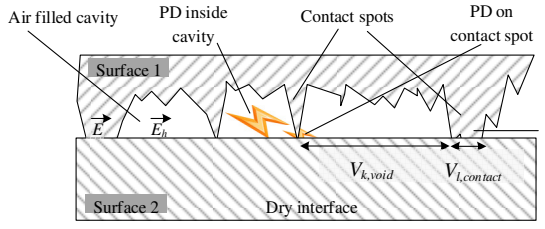

Figure 4. The electrical model of voltage drop at the dry interface where E is the electric field strength on interface, E_h is the field strength inside the voids.

According to the mechanical contact theory in [3, 8], the voids are considered spherical so that a geometrical manipulation is analytically possible. In this way, the of the voids can be determined by calculating the number of voids and the total area that the voids occupy [3]. Regarding the number of voids, another assumption is made; the number of the voids is equal to the number of the contact spots. This assumption is necessary because according to the contact theory only the number of contact spots along the interface be analytically estimated [3, 8].

Equation (2) yields the ratio between the real contact area A_{re} (microscopic) and the nominal contact area A (macroscopic) [8]

$$A_{re} / A \approx 3.2 \frac{p_a}{E' \sqrt{\sigma / \beta_m}} \qquad (2)$$

as a function of the applied contact pressure p_a, the composite elastic modulus of two materials in contact E', the standard deviation of the asperities' heights σ and the mean radius of the asperities' summit β_m [3, 8]. Thus, this formula itself summarizes how the parameters depicted in Figure 2 influence the real contact area, which determines the size of the cavities and eventually the BDS of each cavity according to Paschen's curve (Figure 3). The inception of discharges inside the majority of voids is to be followed simultaneously by breakdown across contact spots [3]. Thus, $\Sigma V_{k,void}$ is the sum of the breakdown voltages of voids at the interface and each depends on the geometry/size of the void (i.e. σ and β_m) together with the gas pressure inside the void.

As discussed in [3, 4], two scenarios are possible for the estimation of gas pressure inside the cavities. First case is the ventilated voids where 100 kPa (1 bar) air pressure (p_0) is retained inside the voids irrespective of the applied pressure. Second case, on the other hand, is the enclosed voids where the air pressure p_0 inside the voids is 100 kPa prior to the application of contact pressure. Then, with the increase of applied pressure, the void diameter d is compressed and hence the pressure inside the voids, p rises proportional to the third-order reduction in d according to (ideal gas law)

$$p = \left(\frac{d_{ref}}{d} \right)^3 p_0 \qquad (3)$$

where d_{ref} is the initial diameter of void when the applied contact pressure p_a is equal to the reference initial applied pressure p_{ref} and p_0 is 100 kPa (see Figure 3). It was shown for the first case that the estimated results agreed well with the measured ones in [3, 4]. On the contrary, in the second case, the difference between the measured and estimated results diverged significantly [3]. Accordingly, the assumption of fixed gas pressure inside the voids was proven to be valid and the gas pressure did not increase while contact pressure was being increased [3, 4]. Therefore, enhanced breakdown voltage against increased contact pressure can be interpreted referring the Paschen's curve at 100 kPa (Figure 3) and the impact of reduced void size can be realized much easier.

Due to the low permittivity of the void compared to the solid, electric field enhancement is likely to cause PD initiation and breakdown of the voids at relatively low voltages. Figure 1 and equation (2) show that the real area of

contact is generally very small compared to the nominal interface area even under heavy mechanical load. Thus, the theoretical estimation of breakdown strength in [3] states that the electric breakdown of one void causes the breakdown of the entire interface promptly since the voltage drop across the contact spots is much lower where they act more as barriers. Hence, the breakdown strength of the interface is considered proportional to the tangential breakdown strength of the interface on which pressure and size of the voids plays a key role according to the Paschen's curve shown in Figure 3. In next sections, experimental results are interpreted using this model to shed light on the effect of contact pressure and modulus on changing the void size at the interface.

3 EXPERIMENT PROCEDURE

This section provides a detailed description of the test setup and the experiment procedure that was followed for the determination of the breakdown strength of solid-solid interfaces for tangentially applied 50 Hz/ac field. As discussed earlier, contact pressure, elastic modulus and surface roughness are the key parameters affecting the void structure that in turn affects the tangential BDS of the interface. Figures 5 and 6 display a detailed sketch of the test setup along with the shape and assembly of the samples. In the experiments, three different contact pressures were applied by using different mechanical loads with XLPE and SiR having different elastic moduli. Quantitatively, the XLPE behaves mechanically similar to the low density polyethylene (LDPE), yielding an elasticity modulus of E_{XLPE} = 470 MPa and a Poisson's ratio of v = 0.5 [9] whereas the elasticity modulus of the silicon rubber is E_{SiR} = 25 MPa with the Poisson's ratio of v=0.48 [14]. The formula to calculate composite elasticity modulus E' in [8, 15] resulted in E'_{XLPE} = 940 MPa for the XLPE-XLPE interface whereas E'_{SiR} = 46 MPa for the SiR-SiR. Evidently, diverse composite elasticity moduli of the interfaces will be of value when the dependency of the breakdown strength on the elasticity is explored.

3.1 TEST SETUP

In order to examine the breakdown strength of solid-solid interfaces under the influence of tangential field, a simple test setup is designed and constructed. Essentially, two rectangular prisms of XLPE or SiR are placed on top of each other (forming the interface) between two vertically placed Rogowski shaped electrodes. The rectangular prisms are 4 mm thick, 55 mm wide and 25 mm tall. The prisms (samples) are pressed against each other vertically, so that the desired contact pressure is achieved. A simple illustration of the core of the test arrangement, as well as the dimensions of the basic components are seen in Figure 5.

The detailed arrangement of the test setup and picture of actual test setup are shown in Figure 6. In the following, the numbers in parentheses refer to Figure 6. The 4 mm-thick rectangular solid specimens (No. 1) made of XLPE or SiR are placed on top of each other forming the interface (No. 2). The two brass electrodes hold the specimens together with the aid of a helical compression spring (No. 5) which pushes the moving electrode (No. 4) against the fixed electrode (No. 3). In this way, the distance between the electrodes is restricted at the width of the specimens. The desired contact pressure at interface is achieved by placing appropriate weights (No. 9) the epoxy made moving weight-carrying plate (No. 10). Different weights are used to achieve the desired pressure levels. Two steel guiding rods (No.11) are used to ensure the stability of the weight carrying plate. The plate applies pressure to the upper pressure dispersing block (no. 12) which moves against the specimens. On the other side, the are restricted by the fixed, lower pressure dispersing block (No. 13). The overall experimental setup is immersed in transformer oil to ensure that the breakdown occurs at the interface. In order to restrict the breakdown current and the transformer, a water resistance is used together with a support insulator.

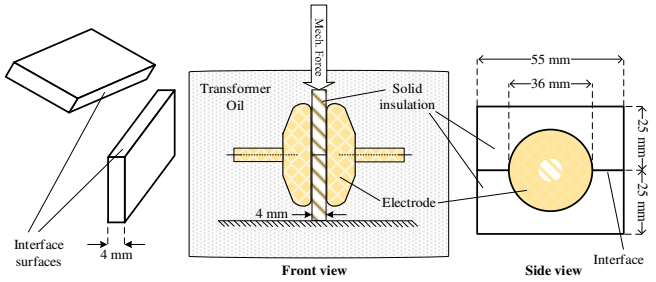

Figure 5. Simple illustration of the test setup. The 4 mm-thick solid insulator samples and the electrodes are depicted with their dimensions.

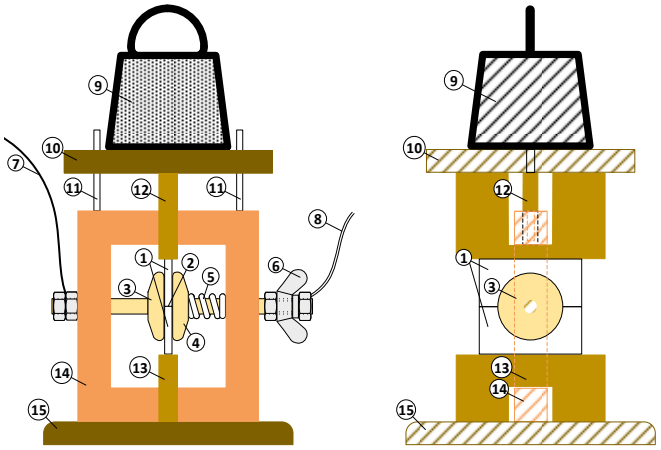

Figure 6. Detailed sketch of the test setup. 1: rectangular solid specimens, 2: interface, 3: fixed electrode, 4: moving electrode, 5: spring, 6: wing nut, 7: high voltage wire, 8: earth wire, 9: weights, 10: weight-carrying plate, 11: guiding rods, 12: moving (upper) pressure dispersing block, 13: fixed (lower) pressure dispersing block, 14: supporting structure, 15: foundation.

3.2 SPECIMEN PREPARATION

All XLPE samples used were cut from the insulation of a commercially available high voltage cable in the size of 4 mm x 55 mm x 25 mm rectangular prisms. The thickness of the samples (i.e. the length of the interface) is 4.0 mm as depicted in Figure 5. We produced all the SiR samples in laboratory conditions. For this purpose, first, we used 4 mm x 500 mm 500 mm sized mold to produce large SiR samples and then we cut them in dimensions of 4 mm x 55 mm x 25 mm

rectangular prisms. The thickness of the samples (i.e. the length of the interface) is 4.0 mm as that of XLPE samples.

3.3 CONTACT SURFACE PREPARATION

Since the surface roughness parameter is to be fixed in this work, all the contact surfaces need to be prepared in the same manner to ensure comparable textures for each experiment. For this purpose, the contact surfaces of both XLPE and SiR samples were made plane and smooth by means of a rotating grinding/sanding disc employing a SiC sandpaper with grit no. 500. During the process, water is continuously being injected on the rotating plane to aid in removing the particles and avoid overheating and deformation of the materials. The samples are sanded for approximately one minute with continuous flow of water so that the produced particles are removed. Subsequently, they are assessed and if necessary, they are sanded further. The prepared samples need to be cleaned and stored until the time they are used. First, the samples are rinsed in tap water and they are left to dry on polyester/cellulose blend cleanroom wipers in a clean, ventilated cupboard. Subsequently, the dry samples are cleaned off particles using filtered compressed air. The clean samples are washed briefly in isopropanol using powder free-latex gloves to avoid recontamination. Finally, the samples are dried using a laboratory drier at approximately 50 °C for 5 minutes. In this way, all the surface humidity is removed. The samples/specimens are now ready and stored in plastic sealed bags until they are used. The interface is subjected to the injection of insulating oil drops with a definite volume (approx. 10 μL) for oil-mate case before it is formed.

Figure 7 shows the measured original surface profiles of both specimens after grinding (using 500 grit no. SiC sandpaper) by means of a 3D optical profilometer (Bruker 3D Optical). The assessment length of the profile is 125 μm, which is about 3% of the total width of interface (4 mm) but a similar behavior for the rest of the surface were observed.

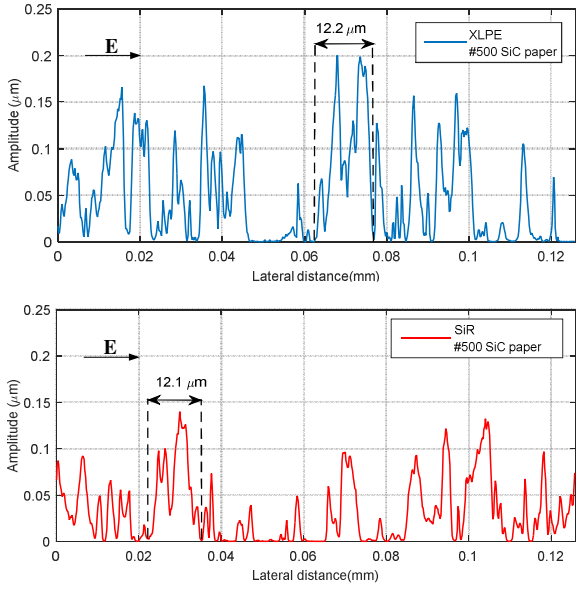

Figure 7. The measured surface roughness profile of XLPE and SiR grinded with a 500 grit no. SiC sandpaper.

These profiles unveil that the max width of interfacial voids of each solid material is almost equal (12.2 μm and 12.1 μm for XLPE and SiR, respectively). Further examination on both the surface textures by the optical profilometer yielded the required motif parameters to be inserted in the roughness and waviness characterization formulas in [5, 15, 16] and subsequently σ and β_m were computed duly and results are tabulated in Table 1.

As mentioned earlier, the roughness parameters are not changed throughout this study (only one type of sandpaper was used), thus merely the resulting roughness/waviness parameters of both materials were calculated and in the discussion section they will be inserted in equation (2) and A_{re}/A will be evaluated under various p_a. To adhere to the focus of this paper, roughness and waviness characterization formulas are not shown explicitly, nor are further details given.

Table 1. Obtained/Calculated Surface Roughness Parameters.

Parameter	Notation	Value		
		XLPE	SiR	Hybrid
Standard deviation of the asperities' heights	σ (μm)	0.041	1.12	0.53
Mean radius of the asperities' summit	β_m (μm)	122	183	153
Composite elasticity modulus	E' (MPa)	940	46	88

Consequently, having examined the surface textures enabled us to obtain the roughness parameters, since as the theoretical model suggests, the air pressure inside the void remains at 100 kPa (1 bar) while its diameter (i.e. width in Figure 7) plays a crucial role on the BDS according to Paschen's curve.

3.4 AC BREAKDOWN TEST

A 100 kV transformer is used to supply the high voltage. The AC voltage at the primary winding of the transformer is regulated by a variac. Considering the expected voltage levels and the number of tests, the voltage rate is chosen to be 1 kV/s. This rate falls within the range of short-time test, as it is defined in ASTM standards [17]. To prevent ingress of oil into the cavities on the interface, surface pressure was applied prior to filling the test chamber with the oil. For each test sample, 7-8 breakdown measurements were made. Each time a new pair of samples was used. The data processing method to evaluate the obtained results is elaborated in the following subsection.

3.5 DATA HANDLING WITH STATISTICAL METHODS

For the analysis of the breakdown data, the Weibull distribution given by

$$P(u) = 1 - \exp\left[-\left(\frac{u-\gamma}{u_{63}}\right)^{\beta}\right] \qquad (4)$$

is employed according to the IEC/IEEE recommendations where u is the breakdown voltage, u_{63} *is* the voltage where 63.2% of the objects broke down (63^{rd} *percentile*), β is the (positive) shape parameter, γ the location parameter

(considered zero in this work, i.e. $\gamma = 0$ yielding a two-parameter Weibull distribution). In the captions of Weibull plots, the shape parameter β and the goodness-of-fit ρ [18] for each curve will be provided. The Weibull cdf, $P(u)$, is often referred to as *unreliability* since $P(u)$ expresses the of breakdown at a voltage equal or lower than u. Throughout each experiment, 2-3 additional experiments were also performed in case of unexpected large deviations occur. Rarely, the breakdown did not happen on the interface but happened between the plates through the insulating oil, especially when the applied voltage had reached to extreme values. In that specific cases, oil might have ingressed to interface due to poor contact peculiar only to those specimens. Yet, these measurements were not disregarded; but considered as censored values and treated accordingly, following the recommendations in [18]. As a result, two types of data emerged, namely complete data and singly censored data whereas only complete data are depicted in the figures.

4 EXPERIMENTAL RESULTS AND DISCUSSION

In this section, the experimental results are presented and the discussions follow promptly. The description of the data handling is given in order to form a basis of understanding. Then, the test results for the dry XLPE-XLPE, SiR-SiR and (XLPE-SiR) hybrid interface are presented and compared. The respective results for the oily interface follow in a similar manner. Chiefly, the results are compared in terms of the *63rd percentile* values (E_{63}) derived from Weibull plots. The *minimum* BDS values (*min*) acquired from each experiment are also contrasted, which is of value in practical cases.

4.1 DRY XLPE-XLPE INTERFACE

First, the breakdown behavior of dry XLPE-XLPE interfaces was examined under three different pressure levels such as 0.5, 0.86 and 1.16 MPa. Figure 8a depicts the Weibull plot of the breakdown strength of the dry samples and Figure 8b illustrates the *min* and *63rd percentile* values for each pressure level. As it is seen, the higher the applied pressure slightly higher the breakdown strength in terms of both (*min* and *63rd percentile*). More specifically, contact pressure increase from 0.5 to 1.16 MPa (i.e. 132% increase) gave rise to a 10% increase in the *min* breakdown strength and 18% in the *63rd percentile* value. This increase might be considered small, yet it confirms the dependency of the BDS on the interfacial pressure of dry mated XLPE samples obviously.

4.2 DRY SiR-SiR INTERFACE

To examine the influence of the elastic modulus on the breakdown strength of solid-solid interfaces, the analogous tests are performed using SiR. The breakdown behavior of dry SiR-SiR interfaces was examined with varying pressure. In case, three different pressure levels, i.e. 0.16, 0.19, 0.27 MPa were used. The pressure levels are considerably lower than that of in the case of XLPE-XLPE due to the more elastic nature of SiR-SiR (i.e. lower E'). It was observed that applied

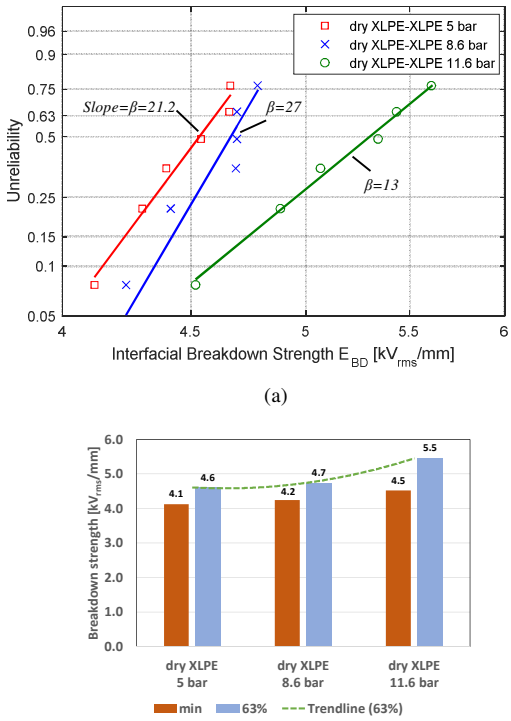

Figure 8. Breakdown strength of dry XLPE-XLPE interface under 0.5 MPa (5 bar), 0.86 MPa (8.6 bar) and 1.16 MPa (11.6 bar) (a) Weibull plot (b) *Minimum* and *63rd percentile* BDS. (ρ=0.99, 0.96, and 0.99, respectively.)

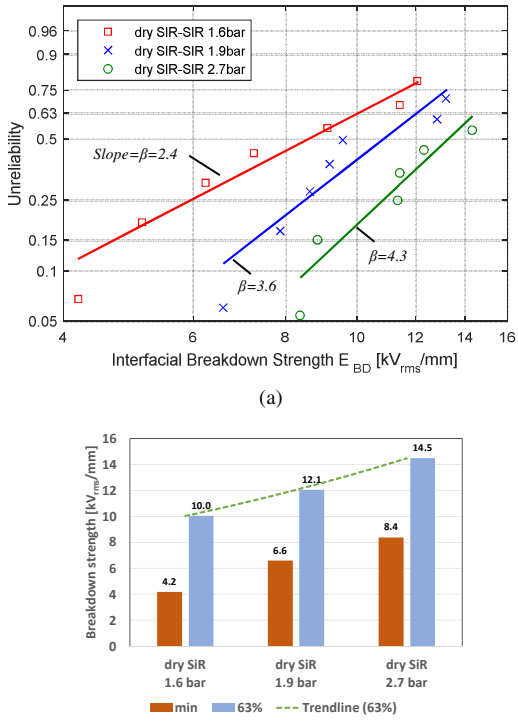

Figure 9. Breakdown strength of dry SiR-SiR interface under 0.16 MPa (1.6 bar), 0.19 MPa (1.9 bar) and 0.27 MPa (2.7 bar) (a) Weibull plot (b) *Minimum* and *63rd percentile* BDS. (ρ=0.97, 0.94, and 0.94, respectively.)

pressure higher than about 0.27 MPa (2.7 bar) was unfeasible because it caused considerable deformation of the rubber. In

Figure 9a, the Weibull plot of the breakdown strength of the dry SiR samples is presented. In addition, Figure 9b illustrates the *min* and *63rd percentile* values for each pressure level in the same manner. As the figures reveal, pressure rise from to 0.27 MPa (1.6 to 2.7 bar i.e. 70% increase) caused a 100% increase in the *min* breakdown value and 44% increase in the *63rd percentile* which clearly verifies that for SiR-SiR interfaces the breakdown strength increases with increasing applied pressure significantly.

4.3 DISCUSSION ON THE IMPACT OF THE ELASTIC MODULUS AND CONTACT PRESSURE

Regarding the results of XLPE-XLPE and SiR-SiR in Figures 8 and 9, the impact of the elastic modulus and the applied contact pressure on the *min* and *63rd percentile* field strength can be revealed. It is evident that the dry SiR-SiR interface performs better than the dry XLPE-XLPE even though the applied pressure is considerably lower. More specifically, the 0.27 MPa (2.7 bar) SiR-SiR dry interface shows a clearly superior behavior compared to the XLPE-XLPE interfaces, despite the higher pressure applied to them. Both indices (*min* and *63rd percentile*) are respectively substantially increased. In the case of dry SiR-SiR interface under 0.16 MPa (1.6 bar), although much higher breakdown strength than the one obtained in dry XLPE-XLPE case (under all pressure levels) is observed, the minimum BDS value turned out to be comparable and was only slightly higher. This indicates that the SiR-SiR dry interface under lower pressure is not necessarily able to withstand higher voltages than the XLPE-XLPE, even though it tends to behave better.

Another observation in Figures 8 and 9 is that the increasing pressure has relatively higher impact on breakdown strength of dry SiR-SiR interfaces than that of XLPE-XLPE. In relation to the experimental results of XLPE-XLPE interface, pressure increase from 0.5 to 1.16 MPa (5 to 11.6 bar), corresponding to an increase of 132%, yields an increase of only 18% in the *63rd percentile* breakdown strength. However, a relatively smaller increase of the pressure applied on the SiR-SiR interface, from 0.16 to 0.27 MPa (1.6 to 2.7 bar i.e. 69%), yields a much higher augmentation in the *63rd percentile* breakdown strength, which is about 44%.

Finally, one significant observation made from Figures 8 and 9 is the higher dispersion of breakdown strength values of SiR-SiR interface compared to XLPE-XLPE interface. In the XLPE-XLPE case, relatively low dispersion of measurements is observed with relative standard deviations of 5% and 8% at 0.5 and 1.16 MPa (5 and 11.6 bar) respectively, which is increasing with pressure. On the other hand, high dispersion is noted for SiR-SiR with relative standard deviations of 39% and 20% at 0.16 and 0.27 MPa (1.6 and 2.7 bar) respectively, which is decreasing with increasing pressure. This leads to the conclusion that for dry SiR-SiR interface, the breakdown strength varies considerably whereas it is much more "predictable" for XLPE-XLPE, in the sense that the lowest highest values are relatively close to each other. The low dispersion in XLPE-XLPE interface and the high dispersion SiR-SiR interface reflects to the values of shape parameter β (i.e. slope of the curves). Thus, it can be inferred that the higher the composite elastic modulus E', the higher the shape parameter β. Last, the calculated values for the goodness-of-ρ (provided in the captions of Figures 8 and 9) proved that all results fit the two-parameter Weibull distribution perfectly consistent with the check curve provided in [18].

4.4 DRY XLPE-SiR (HYBRID) INTERFACE

In this section a hybrid interface is examined. This interface is formed between a SiR and an XLPE sample. The applied pressure was set to 0.27 MPa (2.7 bar). This pressure was the highest pressure level used in the SiR-SiR case, ensuring no deformation of the SiR samples. In Figure 10a, the Weibull plot of the breakdown strength of the dry hybrid interface is shown in comparison with the equivalent XLPE-XLPE and SiR-SiR cases. As evident in Figure 10a, the presence of SiR made a significant difference with a greater measurement dispersion in such a way that the BDS value of the hybrid interface was increased by 43% compared to that of XLPE-XLPE interface whereas it was 39% lower than that of SiR-SiR interface. Yet, it should also be noted that the enhancement in the *min* value (i.e. difference between XLPE-XLPE and hybrid interface) is relatively less compared to that in *63rd percentile* (see Figure 10b). The impact of composite elastic modulus on the shape parameter β is evident in the hybrid interface as well. β was found to be 18.2 for XLPE-XLPE interface, whereas the presence of SiR in hybrid interface made it decrease drastically to 4.3.

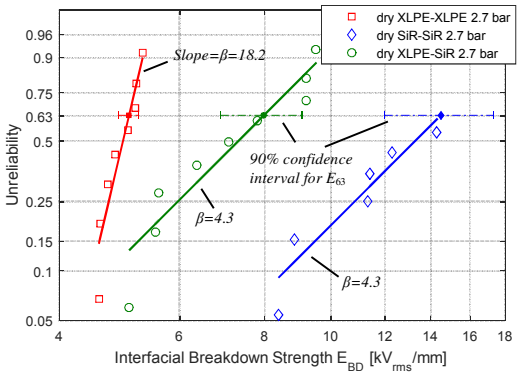

(a)

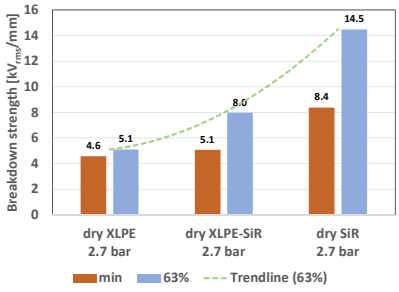

(b)

Figure 10. Breakdown strengths of dry interfaces under 0.27 MPa (2.7 bar) (a) Weibull plot (b) *Minimum* and *63rd percentile* BDS. (ρ=0.95, 0.94 and 0.94, respectively.)

The explanation is as follows: E_{SiR} = 25 MPa with ν = 0.48 whereas E_{XLPE} = 470 MPa with ν = 0.5 yields the composite elasticity modulus of the XLPE and SiR interface as $E'_{XLPE\text{-}SiR}$

≈ 88 MPa. Thus, shape parameter β of the hybrid (XLPE-SiR) and the SiR-SiR interfaces are quite close and the conclusion made in the former section (the higher the E', the higher the β) is further validated. Besides, the 90% confidence limits for *63rd percentile* are shown with error bars in Figure 10a where it lucidly displays that the high dispersion of breakdown strength values in cases where the SiR is present yielded wide bounds of the 90% confidence interval whereas the low dispersion by the XLPE resulted in a quite narrow error bar.

Last, the experimentally obtained E_{63} values for each interface case deliver the mean diameters of d = 0.2204 mm (XLPE-XLPE), d = 0.01974 mm (SiR-SiR) and d = 0.0653 mm (XLPE-SiR) read from the Paschen's curve at 100 kPa (Figure 3). The resulting mean diameter is a useful indicator when assessing the ratio of the real contact area to the nominal contact area (A_{re}/A) as follows. Inserting the parameters in Table 1 into the equation (2) and varying the contact pressure within the range covered in the experiments yields the graphical assessment of the ratio of A_{re}/A shown in Figure 11.

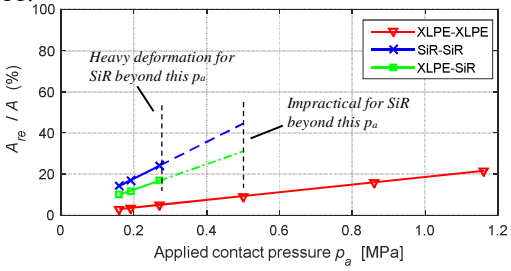

Figure 11. The ratio of the real contact area to the nominal contact area $A_{re}/A(\%)$ under various applied contact pressure p_a (MPa).

Reference [8] shows the multiplication of $\sigma{\cdot}\beta_m{\cdot}\eta$ as constant in the range of 0.03-0.05 where η is the surface density of asperities. Thus, predetermined σ and β_m parameters (see Table 1) for each case deliver $\eta \sim 6{\cdot}10^9$ - $10{\cdot}10^9$ (XLPE-XLPE), $\eta \sim 0.15{\cdot}10^9$ - $0.24{\cdot}10^9$ (SiR-SiR) and $\eta \sim 0.37{\cdot}10^9$ - $0.62{\cdot}10^9$ (XLPE-SiR). Consequently, the lowest ratio of A_{re}/A in XLPE-XLPE case can be attributed to having the biggest mean diameter (lowest E_{63}) with the highest number of asperity density. On the contrary, A_{re}/A ratio in SiR-SiR case is the highest as a result of having the smallest mean diameter (highest E_{63}) with the lowest surface asperity density. Similarly, the ratio of A_{re}/A in the hybrid interface dwells in between due to having medium d and η. Overall, the experimentally obtained values are perfectly in line with the ratios of A_{re}/A provided by the contact theory in Section 2.2.

4.5 LUBRICATED INTERFACE

In this section, the breakdown strength of XLPE-XLPE, SiR-SiR and hybrid interface (XLPE-SiR) assembled with the oil is presented. The interface is subjected to the injection of insulating oil drops with a definite volume (approx. 10 µL) before it is formed/mated. Following, the increasing voltage is applied and the breakdown voltage is recorded. The terms 'lubricated' and 'oily' are used interchangeably describing the injection of insulating oil to the interface before assembly. In Figure 12, the tests were performed for 0.5 MPa (5 bar) XLPE-XLPE, 0.16 MPa (1.6 bar) SiR-SiR and 0.27 MPa (2.7 bar) XLPE-SiR. As evident, the presence of oil in the results in much higher values of breakdown strength, especially in the SiR-SiR case. In some cases such as SiR-SiR at 0.16 MPa (1.6 bar), the breakdown strength of the interface was so high that the breakdown occurred between the plates the oil, not on the interface. This data is then recorded as singly censored data and treated accordingly. The case of SiR-SiR at 0.27 MPa (2.7 bar) was attempted, but no breakdown occurred on the interface. Table 2 tabulates the resulting *63rd percentile* and *minimum* value of BDS, shape factor β and the goodness-of-fit ρ as a result of the obtained Weibull plots for each type of solid material (Figure 12) under indicated contact pressures for both dry and oily interfaces. ρ values proves that results of oily interface also fit the two-parameter Weibull distribution perfectly according to the curve in [18].

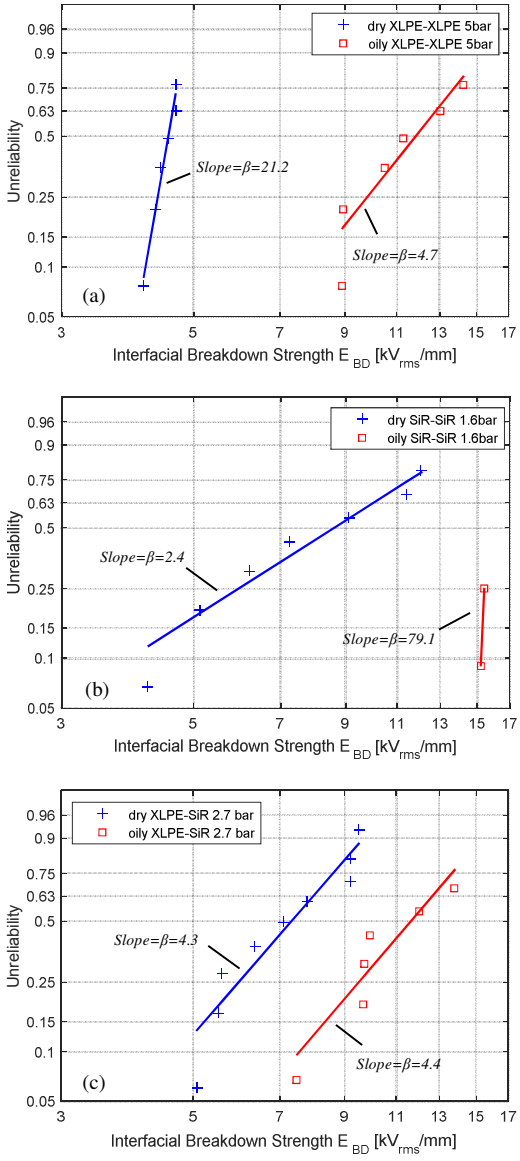

Figure 12. Breakdown strength of dry and oily (a) XLPE-XLPE interface under 0.5 MPa (5 bar) (b) SiR-SiR interface under 0.16 MPa (1.6 bar) (c) XLPE-SiR interface under 0.27 MPa (2.7 bar).

Table 2. Comparison of Oil-filled Cavities vs. Air-filled Cavities.

Interface	p_a [MPa]	E_{63} [kV_{rms}/mm]	*Min BDS* [kV_{rms}/mm]	β	ρ
XLPE-XLPE (dry)	0.5	4.6	4.1	21.2	0.99
XLPE-XLPE (oily)	0.5	12.8	8.9	4.7	0.93
SiR-SiR (dry)	0.16	10.0	4.2	2.4	0.97
SiR-SiR (oily)	0.16	15.7	15.2	79.1	0.99
XLPE-SiR (dry)	0.27	8.0	5.1	4.3	0.95
XLPE-SiR (oily)	0.27	12.7	7.5	4.4	0.95

Figure 13 displays the Weibull plots of breakdown strength of air and transformer oil at 100 kPa (1 bar). Comparison of Figure 13 with those shown in Figure 12 unveils that air enclosed cavities are restraining the dielectric strength of the interface, which is one the most important deductions of this paper. Accordingly, it justifies the adopted theoretical model which assumes ventilated air-enclosed cavities (i.e. 100 kPa) fixed gas pressure inside cavities) and validates the competency of the constructed setup which was successful to prevent oil ingress. Particularly, the Weibull plot of the oily SiR-SiR interface in Figure 12b shows similar behavior to that of transformer oil breakdown tests in Figure 13. Only two experiments out of ten resulted in breakdown on the interface for that case; whereas, the rest occurred between the plates in the oil and were censored in the figure. It unveils the fact that most of the cavities were filled with oil whereas some of the cavities remained empty (air-filled) due to the impact of applied pressure that had removed the oil molecules from those cavities. Therefore, this accounts for the difference between E_{63} values of transformer oil (21.3 kV_{rms}/mm) and oily SiR-SiR interface case (15.7 kV_{rms}/mm).

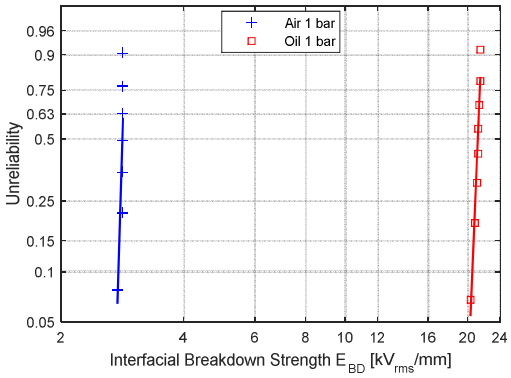

Figure 13. Breakdown strength of air and transformer oil under laboratory conditions at 100 kPa (1 bar). (E_{63} = 2.9 and 21.3 kV_{rms}/mm, respectively.)

Last, interfacial condition after each breakdown test is mentioned here briefly. The energy (heat) released during the electrical breakdown resulted in permanent tracks on the interfacial surface of the specimens. Specific patterns or repeated characteristics of these tracks were observed for each material and/or interface condition. To be more specific, the dry samples of XLPE-XLPE interface are characterized by a clear and clean breakdown path and tree-like incomplete breakdown channels in both sides starting from the edges. The heat evidently caused carbonization of the material and subsequently the specimens were attached. Tree-like channels on the interface were observed and can be attributed to the partial discharge activity which was also noticed during the experiments in the form of audible discharges. These partial discharges had initiated the channels that grew in the forms of both electrical trees and surface tracking paths which become more subtle with the increase of contact pressure. The dry SiR interface has no branches or secondary paths after breakdown implying that the interface withstands the voltage without obvious permanent damage until it breaks down. it can be inferred that SiR shows better mating quality than XLPE while no prominent differences under different levels were observed. Moreover, the characteristic breakdown track for the lubricated XLPE-XLPE and SiR-SiR interfaces are as follows. There were clean and smooth paths which evidently created by local heating of the materials. Having no tree-like tracks and limited carbonization marks imply that the oil restricts the pre-breakdown activity substantially. Therefore, even though a higher field strength is reached, the surface of the specimens was not heavily impaired except for the closest vicinities of the main breakdown path. As a result, it can be argued that the presence of oil on the interface improves not only the breakdown strength but also the overall performance of the interface, since no permanent damage occurred due to the pre-breakdown activity. During tests, the breakdown occurred outside of the interface, it occurred in the oil either on the interface between the upper pressure dispersive block and non-sanded surface of the upper specimen or between the plates along left or right side of the specimens where the minimum creepage distance was present (See Figure 6). In the former case, a deep slit on the non-sanded surface of the upper specimen was observed whereas the latter carbonized oil-molecules arose and stuck to the corresponding edges of the plates.

The assessment of the interfacial conditions suggests that the PD is the precursor phenomenon of the breakdown thus the PD inception stress is also an important factor for designing the high voltage apparatus such as cable joints and terminations. Thus, as a complementary/future study, the PD inception stress will be examined thoroughly and the PD activity will be correlated with the breakdown strength of the interface. In this regard, the PD will be observed whether it starts simultaneously in each cavity or in the largest cavity first and thus the contact theory model will be improved duly.

5.CONCLUSION

Although the starting point of this work is the existing wet-mate cable connector technology, the study of solid-solid interfaces is beneficial for any insulating equipment cable joints and terminations. To start with, dry SiR-SiR interface showed higher BDS despite the much lower applied pressure compared to dry XLPE-XLPE interface. These together with the hybrid interface results concluded that the presence of SiR had made a significant improvement in BDS since a more elastic material (lower E) results in smaller in turn yielding higher BDS in line with Paschen's curve. However, BDS values of SiR-SiR interface disclosed wider dispersion that increases the uncertainty when designing

equipment. This dispersion supported the conclusion that the higher the composite elastic modulus E', the higher the shape parameter β in Weibull distribution resulting in much wider 90% confidence limits. In addition, the superiority of the lubricated interface regardless of the material was shown through experimental testing. Especially the SiR-SiR interface showed exceptional performance, in some cases breakdown occurred between the plates in the oil, not on the interface. hypothesis is made such that the insulating oil fills the on the interface and hence the BDS is improved significantly. Thus, air-filled cavities are the limiting factor in the overall dielectric strength of the interface and the injection of insulating liquids/gels prior to mating is of vital value in practical applications to ensure high breakdown strength and long service duration. Besides, tree-like tracking on the surface of the samples reveals pre-breakdown activity that fits to the concept of cavity induced breakdown supported by the contact theory. In terms of the ratio of the real contact area to the nominal contact area (A_{re}/A) yielded by the contact theory and surface profilometer measurements, SiR-SiR, XLPE-SiR and XLPE-XLPE are ordered from the best to the worst in a sequence which is in accordance with the experimentally obtained breakdown strength values.

ACKNOWLEDGMENT

The authors express deepest gratitude for the financial support of the Norwegian Research Council and SINTEF Energy Research and appreciate the guidance provided by the senior researcher Dr. Sverre Hvidsten.

REFERENCES

[1] S. Midttveit, B. Monsen, S. Frydenlund, and K. Stenevik, "SS on Implications of subsea processing power distribution-subsea power systems-a key enabler for subsea processing," Offshore Technology Conf., 2010.

[2] P. Weiss, S. Beurthey, Y. Chardard, J.-F. Dhedin, T. Andre, K. Rabushka, et al., "Novel wet-mate connectors for high voltage and power transmissions of ocean renewable energy systems," 4th Int'l. Conf. Ocean Energy, 2012.

[3] S. M. Hasheminezhad, E. Ildstad, and A. Nysveen, "Breakdown strength of solid|solid interface," IEEE 10th Int'l. Conf Solid Dielectr. (ICSD), pp. 1-4, 2010.

[4] S. M. Hasheminezhad, "Breakdown strength of solid| solid interfaces," IEEE PowerTech, Trondheim, Norway, pp. 1-7, 2011.

[5] M. Hasheminezhad and E. Ildstad, "Application of contact analysis on evaluation of breakdown strength and PD inception field strength of solid-solid interfaces," IEEE Trans. Dielectr. Electr. Insul., Vol. 19, pp. 1-7, 2012.

[6] S. E. Research. High Voltage Subsea Connection [Online]. Available: https://www.sintef.no/en/projects/subsea-power-supply/

[7] D. Fournier and L. Lamarre, "Interfacial breakdown phenomena between two EPDM surfaces," 6th Int'l. Conf. Dielectr. Materials, Measurements and Applications, pp. 330-333, 1992.

[8] B. Bhushan, "Analysis of the real area of contact between a polymeric magnetic medium and a rigid surface," J. Tribology, Vol. 106, pp. 26-34, 1984.

[9] D. Gracias and G. Somorjai, "Continuum force microscopy study of the elastic modulus, hardness and friction of polyethylene and polypropylene surfaces," Macromolecules, Vol. 31, pp. 1269-1276, 1998.

[10] D. Fournier and L. Lamarre, "Effect of pressure and length on interfacial breakdown between two dielectric surfaces," IEEE Int'l. Sympos. Electr. Insul., pp. 270-272, 1992.

[11] D. Fournier, C. Dang, and L. Paquin, "Interfacial breakdown in cable joints," IEEE Int'l. Sympos. Electr. Insul., pp. 450-452, 1994.

[12] T. Takahashi, T. Okamoto, Y. Ohki, and K. Shibata, "Breakdown strength at the interface between epoxy resin and silicone rubber-a basic study for the development of all solid insulation," IEEE Trans. Dielectr. Electr. Insul., Vol. 12, pp. 719-724, 2005.

[13] B. X. Du, L. Gu, Z. Xiangjin, and Z. Xiaohui, "Fundamental research on dielectric breakdown between XLPE and silicon rubber interface in HV cable joint," IEEE 9th Int'l. Conf. Properties and Applications of Dielectr. Materials (ICPADM), pp. 97-100, 2009.

[14] D. R. Askeland and P. P. Phulé, *The science and engineering of materials*: Springer Netherlands, 2003.

[15] S. Belghith, S. Mezlini, H. BelhadjSalah, and J.-L. Ligier, "Modeling of contact between rough surfaces using homogenisation technique," Comptes Rendus Mécanique, Vol. 338, pp. 48-61, 2010.

[16] F. Robbe-Valloire, "Statistical analysis of asperities on a rough surface," Wear, Vol. 249, pp. 401-408, 2001.

[17] ASTM, "Standard test method for dielectric breakdown voltage and dielectric strength of solid electrical insulating materials at commercial power frequencies," Technical Report, West Conshohocken, PA1994.

[18] "IEC/IEEE Guide for the Statistical Analysis of Electrical Insulation Breakdown Data (Adoption of IEEE Std 930-2004)," IEC 62539 First Edition 2007-07 IEEE 930, pp. 1-53, 2007.

Emre Kantar (M'14) received the B.Sc. and M.Sc. degrees in electrical engineering from Middle East Technical University, Ankara, Turkey, in 2011 and 2014, respectively. From 2010 to 2014, he was with Aselsan, Inc., Ankara and worked as an R&D engineer. He is currently a Ph.D. candidate at the Department of Electric Power Engineering, Norwegian University of Science and Technology, in Trondheim, Norway. His research interests include power electronics, renewable energy, subsea connectors and high voltage equipment and insulation materials.

Dimitrios Panagiotopoulos received the B.Sc. degree in electrical and computer engineering from National Technical University of Athens, Athens, Greece, in 2011. Since 2013, he is pursuing his double M.Sc. in electrical engineering and technology-wind energy at the Technical University of Delft (TU Delft) and the Norwegian University of Science and Technology (NTNU) respectively. His research interest is in high voltage equipment, electrical machines, and control of electrical drives, power systems and wind energy.

Erling Ildstad received the M.Sc. degree in technical physics in 1978 and the Ph.D. degree in electrical power engineering in 1982 from the Norwegian University of Science and Technology (NTNU) in Trondheim, Norway. Since then his main research activity has been related to the development and testing of insulation systems for ac and dc power cables. He has been a full-time professor of high voltage engineering at NTNU since 1993, and has been the head of the Electric Power Engineering Department from 1998 to 2008 and 2011 onward.